

ON THE BRANCHING GEOMETRY OF ALGEBRAIC FUNCTIONS

DOMINIC C. MILIOTO

ABSTRACT. This paper describes an algorithm for determining the branching geometry of algebraic functions. The graphs of these complex-valued functions have a complicated interweaving structure that can be described by analytic branches separated by singular points. Power expansions for the branches in discs centered at a point can be computed using the Newton Polygon method, and expansions around annular regions centered at the origin computed using a version of Laurent's Theorem applied to algebraic functions. However, neither of the methods enable a determination of the region of convergence of the power series. In this paper, a method using analytic continuation is used to determine the domain of analyticity for the branches, and the Root Test used to numerically check the results.

The software used to implement the algorithm is Mathematica ver. 11.1.

1. INTRODUCTION

The objects studied in this paper are algebraic functions $w(z)$ expressed implicitly by the equation

$$f(z, w) = a_0(z) + a_1(z)w + a_2(z)w^2 + \cdots + a_n(z)w^n = 0, \quad (1)$$

with z and w complex variables and the coefficients, $a_i(z)$, polynomials in z with rational coefficients. The degree of the function is the highest power of w . By the Implicit Function Theorem, this equation defines locally, an analytic function $w(z)$ when $\frac{\partial f}{\partial w} \neq 0$. And it is known from the general theory of algebraic functions that the solution, $w(z)$, has n fractional power series expansions about a point. These fractional power series can be computed by the Newton polygon method and often have finite radii of convergences determined by the nearest impinging singular point so do not in general represent the entire function. Power series for annular regions are also fractional and can be computed by a version of Laurent's Theorem applied to algebraic functions.

The purpose of this paper is four-fold:

- (1) Describe an algorithm to determine the branching geometry of an algebraic function,
- (2) Describe a method of applying Laurent's Theorem to compute annular power series expansions of an algebraic function,
- (3) Determine the region of convergence of a fractional power series representation of $w(z)$,
- (4) Present a software tool for visually investigating the branching of algebraic functions.

2. SOME PROPERTIES OF ALGEBRAIC FUNCTIONS USED IN THIS PAPER

Fractional power expansions of algebraic functions are called Puiseux series and usually have finite radii of convergences. As stated earlier, series centered at a point can be computed by the Newton Polygon method but usually represent a small portion of (1). Power series for annular regions can in principle, be computed using a variation of Laurent's Theorem for multivalued functions. The Laurent expansions computed this way are again fractional power expansions. In this way, the global branching geometry of $w(z)$ can be represented in the form of singular points segregating the z -plane into annular regions where the function is analytic and ramifies into multivalued branches. This branching, both around the singular points and annular regions, are represented by the notation $\{s_1, s_2, \cdots, s_n\}$ where each s_i represents an analytic and single-valued sheet of the branch. For example the notation $\{1, 2\}$ represents a 2-cycle branch, such as \sqrt{z} , and the numbers 1 and 2 represent the sort order of the function value at predetermined points

Date: March 8, 2021.

2010 Mathematics Subject Classification. Primary 14O1, 30B10; Secondary 30B50, 30B40.

Key words and phrases. Puiseux series, fractional power series, algebraic functions, radius of convergence, Newton-polygon.

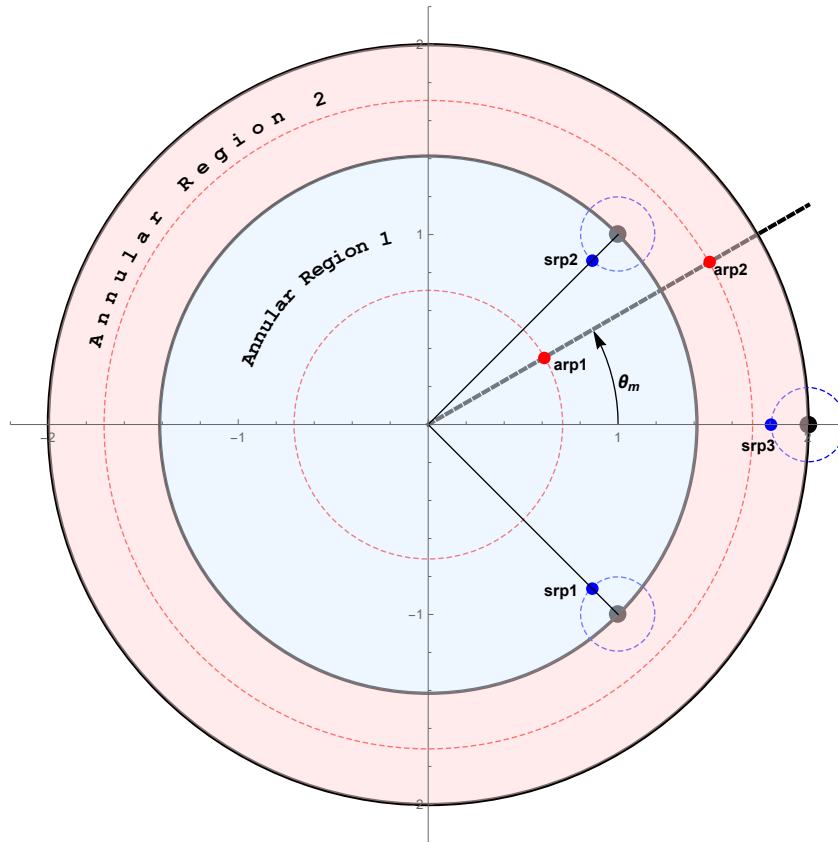


FIGURE 1. Annular Regions and Integration Paths

in the z -plane called the annular or singular point reference point. Figure 1 shows these points as the blue and red dots labeled ‘arp’ and ‘srp’.

The Resultant of $f(z, w)$ with it’s derivative f_w is denoted by $R(f, f_w)$. A point z where $R(f, f_w)$ is zero is a singular point of f . However this does not tell us which branch sheet is singular. A point where $a_n(z) = 0$ is a pole, possibly ramified. Singular points are sorted first by the real component and then the imaginary component and labeled s_n with n ranging from one to the total number of singular points including the point at infinity. Even though the function may not ramify and thus not be singular at infinity we still include it in the list of singular points.

A singular point may not affect all coverings of an algebraic function unless the function fully-ramifies at the singular point. For example, a 10-degree function may only ramify into a single 2-cycle branch at a singular point with the remaining coverings single-cycled and unramified. In this case, the 2-cycle covering is singular. The eight single-cycle coverings are not analytically affected at this singular point unless one is affected by a pole of the function. However, if the function fully-ramifies into a 10-cycle branch at this singular point, all coverings would be affected. It is for this reason a power expansion of an algebraic function often has a region of convergence extending beyond the nearest singular point: the branch coverings may simply not be affected by the singular point. Only when the covering becomes singular does the convergence region of its power expansion become established. The main objective of this paper is to identify which singular point is interrupting the analyticity of branch cycles thereby establishing the region of convergence of their power expansions.

The following conventions are used in this paper:

- (1) The Puiseux expansions of (1) consist of a set of d -valued branches. A branch is sometimes called a d -cycle where d is a positive integer. A power series in $z^{1/3}$ would be a 3-cycle branch. It has three coverings over the complex z -plane similar to $\sqrt[3]{z}$. The sum of the cycles is always equal to the degree of the function in w .
- (2) The concept of “branch” is used throughout this paper and refers to a multi-valued d -cycle of $w(z)$.

- (3) The following discussion makes use of the term, “extending a branch over a singular point”. This is in reference to the discussion above about singularities and the coverings they affect.
- (4) r_c is a positive integer representing the radius of a circular ring with center at the origin. These rings are created by arranging the finite singular points in order of increasing absolute value. The smallest non-zero singular point is therefore on ring one with radius r_1 . Singular points with the next largest absolute value are on ring two of radius of r_2 and so forth.
- (5) We further sub-divide singular points into function singular points and branch singular points. The function singular points is the solution set to $R(f, f_w) = 0$ as discussed above. A branch singular point is a singular point impinging one or more branch sheets, and this is done to emphasize singular points often do not affect all branches. For example, if singular point s_i is on a 3-cycle branch, then s_i becomes the branch singular point. Other cycles may not be affected by this singular point and so s_i is not a branch singular point for these cycles.
- (6) Power series for algebraic branches are fractional power series called Puiseux series. Two methods are used to compute these power series: Newton Polygon and Laurent’s Theorem applied to algebraic functions. For brevity, only a few terms of a series are listed. Actual computations for this paper used up to 1024 terms with over 4000 digits of precision.

3. DETERMINING MONODROMIES

We first compute the finite singular points of the function by setting the resultant, $R(f, f_w)$, equal to zero. This gives a list of z values where the singular points are located. We then sort the points in order of absolute value creating rings around the origin. In the annular regions between rings, the function is analytic and splits into multi-valued branches.

Our next objective is to determine the branching geometry around each singular point and each annular region. We then determine the annular domain of analyticity for each annular branch. The branching is called monodromy or ‘ramified covering’ and we use these terms interchangeably. The monodromy is computed by numerical integration: If we follow an analytically-continuous 2π circular path over a branch covering around a singular point enclosing no other singular point, then at the end of the path, we may or may not return to the same starting point on the branch. If we return to the same value, we have identified a single-cycle branch. If we need to traverse a 4π circuit to return to the same starting point, then we have traversed a 2-cycle branch and so forth. In practice however, we use a somewhat different algorithm but the principle is similar. This give us the local monodromy around the singular point. And we use the same approach to determine the monodromy of each annular region. Naturally, this requires a comparison of floating-point numbers and some type of numerical accuracy must be established to identify terms considered identical. We check a certain number of digits to the right of the decimal place without rounding. For example, we could require five digits of accuracy between $w(0)$ and $w(2\pi)$ to be considered equal. However care must be take to avoid rounding or cases when we have for example 0.999999999. We can check the later case and convert it to 1 in order to check the values.

Consider first the function

$$f(z, w) = w^2 - (z - (1 + i))^2(z - (1 - i))^2(z - 2) = 0. \quad (2)$$

Setting $R(f, f_w) = 0$ we obtain as the singular points, $\{1 - i, 1 + i, 2, \infty\}$ and the rings in Figure 1. The black circles demarcate the annular regions separated by one or more singular points shown in the figure as black dots. During the analysis, we integrate around annular regions and singular points beginning at reference points labeled ‘arp’ in the figure for annular regions and ‘srp’ for singular points. The annular integration paths are shown as the red dashed circles. The blue dashed circles are the singular point integration paths.

As stated, we use numerical integration over 2π routes around each annular region to determine the monodromy. And in order to minimize errors we take a route with a mean radius of each region to maximize the distance to the nearest singular point. For example, if a region was given by $1 \leq r \leq 2$, we would integrate at 1.5 using $z(t) = 1.5e^{it}$. But how do we decide if values are identical? We can do this by extracting a set number of decimal digits. For example, consider the value $1.23901950708 - 0.278993512i$.

Taking an accuracy of 5 digits, we construct the following approximate integer representation of this number:

$$((1, (1, 2, 3, 9, 0), 1), (-1, (2, 7, 8, 9, 9), 0)),$$

with the format $\{s, \{d_1, d_2, \dots, d_n\}, e\}$ with s being the sign of the number, (d_1, d_2, \dots, d_n) the digits of the number and e being the number of digits to the left of the decimal place. Notice that we did not round the number. So we basically convert a floating point number to an integer sequence so that we can make exact comparisons of floating point numbers up to a desired accuracy. In practice, we are comparing a number against a set of numbers and we check that the smallest difference between the set of numbers is larger than the accuracy of the comparison to minimize errors.

Now consider a 10-degree algebraic function. We wish to integrate over one of the annular regions and then compare the starting and ending values of the function over each 2π route of each branch sheet. Table 1 gives actual results for a 10-degree function. Looking carefully at the starting and ending values we see the w_1 root goes back to the w_1 root so this is a single cycle branch $\{1\}$. Next, the w_2 root goes to w_7 then w_6 then w_4 back to w_2 . This is a 4-cycle branch, $\{2, 7, 6, 4\}$. We then have two single cycle branches w_3 and w_5 , then a 3-cycle branch w_8, w_9, w_{10} . Therefore the annular monodromy is

$$\{\{1\}, \{2, 7, 6, 4\}, \{3\}, \{5\}, \{8, 9, 10\}\}.$$

TABLE 1. Monodromy digits

Root	Starting Value	Ending Value
1	$(((-1, (1, 0, 5, 0, 8), 1), (-1, (4, 0, 8, 8, 9), -1))$	$(((-1, (1, 0, 5, 0, 8), 1), (-1, (4, 0, 8, 8, 9), -1))$
2	$(((-1, (4, 7, 6, 5, 7), 0), (-1, (1, 9, 8, 2, 8), -1))$	$((1, (5, 8, 2, 9, 7), 0), (1, (9, 7, 6, 1, 3), 0))$
3	$(((-1, (4, 0, 9, 0, 9), 0), (1, (7, 3, 5, 4, 2), 0))$	$(((-1, (4, 0, 9, 0, 9), 0), (1, (7, 3, 5, 4, 2), 0))$
4	$(((-1, (2, 5, 8, 4, 2), 0), (-1, (1, 3, 8, 2, 8), 1))$	$(((-1, (4, 7, 6, 5, 7), 0), (-1, (1, 9, 8, 2, 8), -1))$
5	$(((-1, (2, 3, 9, 4, 1), 0), (-1, (7, 6, 4, 2, 7), 0))$	$(((-1, (2, 3, 9, 4, 1), 0), (-1, (7, 6, 4, 2, 7), 0))$
6	$(((-1, (3, 8, 0, 2, 3), -1), (1, (7, 0, 9, 5, 3), -1))$	$(((-1, (2, 5, 8, 4, 2), 0), (-1, (1, 3, 8, 2, 8), 1))$
7	$((1, (5, 8, 2, 9, 7), 0), (1, (9, 7, 6, 1, 3), 0))$	$(((-1, (3, 8, 0, 2, 3), -1), (1, (7, 0, 9, 5, 3), -1))$
8	$((1, (9, 5, 0, 3, 7), 0), (-1, (4, 4, 9, 0, 4), 0))$	$((1, (1, 1, 0, 7, 5), 1), (-1, (5, 2, 0, 1, 7), -1))$
9	$((1, (1, 1, 0, 7, 5), 1), (-1, (5, 2, 0, 1, 7), -1))$	$((1, (1, 1, 4, 4, 9), 1), (1, (6, 2, 4, 2, 6), 0))$
10	$((1, (1, 1, 4, 4, 9), 1), (1, (6, 2, 4, 2, 6), 0))$	$((1, (9, 5, 0, 3, 7), 0), (-1, (4, 4, 9, 0, 4), 0))$

4. NUMERICALLY SOLVING THE MONODROMY DIFFERENTIAL EQUATIONS

In order to determine monodromies, we integrate over the function around each annular region and around each singular point. We do this by solving the monodromy differential equation: Given $f(z, w) = a_0(z) + a_1(z)w + \dots + a_n(z)w^n = 0$, we have $\frac{dw}{dt} = -\frac{f_z}{f_w} \frac{dz}{dt}$ which is a first-order differential equation. In order to compute the monodromy, we can solve this differential equation for $w(t)$ over a circular path around annular regions and singular points. For example, we would solve the following n initial value problems for a function of degree n :

$$\frac{dw}{dt} = -\frac{f_z}{f_w} \frac{dz}{dt}, \quad (z_0, w_i), \quad i = 1, 2, \dots, n$$

where w_i are the roots to the expression $f(z_0, w) = 0$. We then compile the values of $w(t)$ at the beginning and ending of each 2π route. However, in order to obtain accurate results, we will have to adjust the working precision and step size of the numerical integration as needed to achieve the desired accuracy. To economize this, we set up a loop of decreasing step size with increasing precision ranging from $(1/1000, 20)$ to $(1/50000, 65)$. However, even at the high range of precision, we may not be able to resolve the branching if for example the region is very small or the branch sheets are very close to each other. For random functions, we have found if the annular size, $|r_2 - r_1|$, is larger than $1/5000$, and the difference between

branch sheets is greater than the desired accuracy, then a 10-degree function can usually be processed successfully. Therefore, this paper deals only with functions of degree 10 or less with $|r_2 - r_1| \geq 1/5000$.

5. DETERMINING THE BRANCHING GEOMETRY

We divide this section into the following sub-sections:

- (1) Computation of singular points,
- (2) Construction of annular regions,
- (3) Compute singular point monodromies,
- (4) Compute annular monodromies,
- (5) Determine branch-continuation support,
- (6) Compute branch continuations.
- (7) Determine continuations over poles,

and use the following function to illustrate the concepts:

$$f(z, w) = (9) + (-7)w + (7 - 2z - 4z^2 - z^3)w^2 + (7z - 2z^3)w^3. \quad (3)$$

TABLE 2. Singular points

Singularity	Value
s_1	0.
s_2	-0.21713-0.255535 i
s_3	-0.21713+0.255535 i
s_4	1.36571
s_5	-1.83037-0.0204249 i
s_6	-1.83037+0.0204249 i
s_7	-1.87083
s_8	1.87083
s_9	2.21932 -1.22168 i
s_{10}	2.21932 +1.22168 i
s_{11}	-6.85468-6.05671 i
s_{12}	-6.85468+6.05671 i
s_{13}	∞

5.1. Computation of singular points. Using the built-in Mathematica function `NSolve`, the finite singular points are easily determined. However, in order to later compute successfully the annuli and singular monodromies, we need to compute the singular points at a sufficiently high precision. In this paper, we do so at 75 digits of precision and we attempt to carry approximately, this precision throughout the calculations. Table 2 lists the singular points in blue where we have identified poles in red.

5.2. Construction of rings and annular regions. Once the singular points are computed, they are arranged in order of increasing absolute values which then segregate the z -plane into annular regions separated by rings. On each ring lies one or more singular points. Table 3 lists the rings, r_i , which will become the regions of convergence of the power expansions of each function branch computed below. For example, a branch may have a region of convergence given by (r_1, r_3) .

Between each ring are annular region devoid of singular points. Table 4 lists the annular regions separated by the ring singular points. The last region is simply determined by an arbitrary distance from the most distant finite singular point. In this case, this distance is 4.

TABLE 3. Rings and Singular points

Ring	Radius	Singularity	Value
r_1	0.335327	s_1	-0.21713 - 0.255535 i
		s_2	-0.21713 + 0.255535 i
r_2	1.36571	s_3	1.36571
r_3	1.83048	s_4	-1.83037 - 0.0204249 i
		s_5	-1.83037 + 0.0204249 i
r_4	1.87083	s_6	-1.87083
		s_7	1.87083
r_5	2.53336	s_8	2.21932 - 1.22168 i
		s_9	2.21932 + 1.22168 i
r_6	9.14715	s_{10}	-6.85468 - 6.05671 i
		s_{11}	-6.85468 + 6.05671 i

TABLE 4. Annular Regions

Annulus	Annulus/singular point
	0.
c_1	{0.00005, 0.335277} -0.21713-0.255535 i -0.21713+0.255535 i
c_2	{0.335377, 1.36566} 1.36571
c_3	{1.36576, 1.83043} -1.83037-0.0204249 i -1.83037+0.0204249 i
c_4	{1.83053, 1.87078} -1.87083 1.87083
c_5	{1.87088, 2.53331} 2.21932 - 1.22168 i 2.21932 + 1.22168 i
c_6	{2.53341, 9.1471} -6.85468-6.05671 i -6.85468+6.05671 i
c_7	{9.1472, 13.1471} ∞

5.3. Computation of annular monodromies. With annular regions defined, we next compute the annular monodromies. One way to compute this is to simply integrate around annuli over 2π routes, one route for each branch sheet for a total of n sheets and determine how many routes to return to a starting point as was shown above in Table 1 until all the branch sheets have been processed. This necessarily involves comparing floating-point numbers, but if we are willing to accept a tolerance say of five decimal digits to the right of the decimal point or other numerical accuracy, experience has shown we can obtain reliable results. As stated earlier, to effect this integration, we integrate the monodromy differential equation. In the case of the annular regions, we choose a circular path midway in the region with starting value $z(\theta_0)$ with θ_0 chosen somewhat arbitrarily to best effect the integration. For example, θ could be chosen to maximize the distance from most singular points. We then form a table of starting and ending values as described in Section 3 above for each path and then determine the monodromies through integer comparisons. This gives us the monodromy results in Table 5.

TABLE 5. Annular Monodromies

Annulus	Annulus/singular point	Monodromies
	0.	
c_1	{0.00005,0.335277} -0.21713-0.255535 i -0.21713+0.255535 i	((1),(2),(3))
c_2	{0.335377,1.36566} 1.36571	((1,3,2))
c_3	{1.36576,1.83043} -1.83037-0.0204249 i -1.83037+0.0204249 i	((1,3),(2))
c_4	{1.83053,1.87078} -1.87083 1.87083	((1,2),(3))
c_5	{1.87088,2.53331} 2.21932 -1.22168 i 2.21932 +1.22168 i	((1,2),(3))
c_6	{2.53341,9.1471} -6.85468-6.05671 i -6.85468+6.05671 i	((1,2),(3))
c_7	{9.1472,13.1471}	((1),(2,3))
	∞	

5.4. Computing singular point monodromies. The procedure for computing singular point monodromies is identical to that for the annular regions: We solve the monodromy DE for a circular path around each singular point containing no other singular points. In the case of the monodromy around infinity, we integrate over a closed contour enclosing all finite singular points. These results are shown in Table 6.

5.5. Determining support. Now that we have the monodromies for both the annular regions and singular points, we can determine the possible support of each annular branch across intervening singular points. A necessary condition for branch continuation across a singular point is that that singular monodromy between successive annuli must support a sufficient number of single-cycle branches to continue the branch into the next annular region. For example, if we are considering extending a 3-cycle branch across a singular point, then the monodromy around this singular point must have three single-cycle branches. And likewise for other cycles.

A second necessary condition is that the next or post-annular monodromy must have the same branch cycle type we are attempting to continue. Table 7 shows the possible branch continuations. For example, consider the first and second annuli in Table 7 and the intervening singular points: The first annulus has three single-cycle branches. In order to continue one or more of these branches into annulus two, the singular points between these regions must support single-cycle branches. In this case, the singular points do have single-cycle branches. However, annulus 2 is fully-ramified into a 3-cycle branch so does not support continuing any of the single-cycle branches. And likewise for annulus 2: In order to continue this branch into annulus 3, we would need three single-cycle branches over the intervening singular points. In the case of annulus 3 with monodromy $\{\{1, 3\}, \{2\}\}$, we cannot continue the 2-cycle branch into annulus 4 since the intervening singular points do not support two single-cycle branches. However there is support to continue branch $\{2\}$: the singular point has a single-cycle branch and annulus 4 does as well. Now consider annuli 4 and 5 and the two poles between them: the poles do not ramify but rather consists of three single-cycle branches and so supports continuing both the $\{1, 2\}$ branch and the $\{3\}$ branch however not holomorphically: one or more of the branches will contain a pole.

TABLE 6. Annular and Singular Point Monodromies

Annulus	Annulus/singular point	Monodromies
	0.	$((1),(2),(3))$
c_1	{0.00005,0.335277}	$((1),(2),(3))$
	-0.21713-0.255535 i	$((1),(2,3))$
	-0.21713+0.255535 i	$((1),(2,3))$
c_2	{0.335377,1.36566}	$((1,3,2))$
	1.36571	$((1),(2,3))$
c_3	{1.36576,1.83043}	$((1,3),(2))$
	-1.83037-0.0204249 i	$((1),(2,3))$
	-1.83037+0.0204249 i	$((1),(2,3))$
c_4	{1.83053,1.87078}	$((1,2),(3))$
	-1.87083	$((1),(2),(3))$
	1.87083	$((1),(2),(3))$
c_5	{1.87088,2.53331}	$((1,2),(3))$
	2.21932 -1.22168 i	$((1,2),(3))$
	2.21932 +1.22168 i	$((1,2),(3))$
c_6	{2.53341,9.1471}	$((1,2),(3))$
	-6.85468-6.05671 i	$((1,2),(3))$
	-6.85468+6.05671 i	$((1,2),(3))$
c_7	{9.1472,13.1471}	$((1),(2,3))$
	∞	$((1),(2,3))$

TABLE 7. Support

Annulus	Annulus/singular point	Monodromies	Support
	0.	$((1),(2),(3))$	
c_1	{0.00005,0.335277}	$((1),(2),(3))$	
	-0.21713-0.255535 i	$((1),(2,3))$	
	-0.21713+0.255535 i	$((1),(2,3))$	
c_2	{0.335377,1.36566}	$((1,3,2))$	
	1.36571	$((1),(2,3))$	
c_3	{1.36576,1.83043}	$((1,3),(2))$	$((2))$
	-1.83037-0.0204249 i	$((1),(2,3))$	
	-1.83037+0.0204249 i	$((1),(2,3))$	
c_4	{1.83053,1.87078}	$((1,2),(3))$	$((1,2),(3))$
	-1.87083	$((1),(2),(3))$	
	1.87083	$((1),(2),(3))$	
c_5	{1.87088,2.53331}	$((1,2),(3))$	$((3))$
	2.21932 -1.22168 i	$((1,2),(3))$	
	2.21932 +1.22168 i	$((1,2),(3))$	
c_6	{2.53341,9.1471}	$((1,2),(3))$	$((3))$
	-6.85468-6.05671 i	$((1,2),(3))$	
	-6.85468+6.05671 i	$((1,2),(3))$	
c_7	{9.1472,13.1471}	$((1),(2,3))$	
	∞	$((1),(2,3))$	

5.6. Determining branch continuations. In the previous section, we defined a necessary condition for branch continuation: The intervening singular points must support continuation. A sufficient condition is that each branch sheet be analytically continuous over all singular points on the bordering ring and

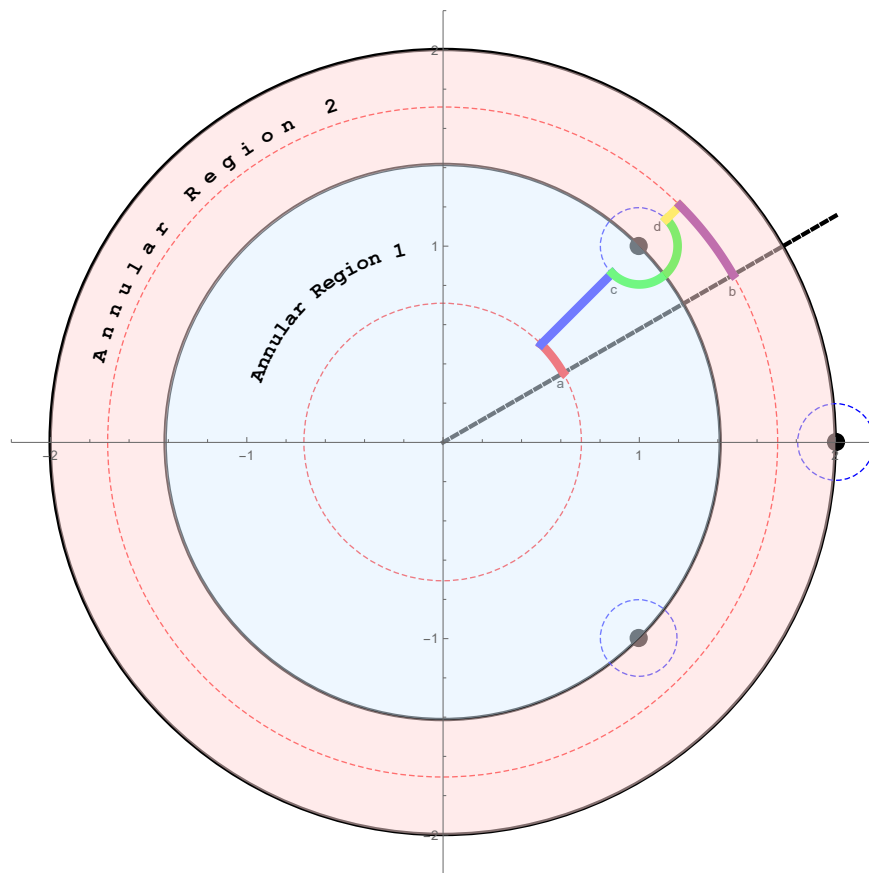


FIGURE 2. Continuation Path

continuing into the next annular region onto a branch with the same monodromy sequence. For example, if we are attempting to continue a 3-cycle branch $\{2, 1, 3\}$ across a singular point from annulus k to annulus $k + 1$, then from above, the singular monodromy must support three single-cycle branches, and annulus $k + 1$ must have a 3-cycle branch such as $\{1, 2, 3\}$ such that sheet 2 in annulus k is continued onto sheet 1 of annulus $k + 1$, sheet 1 is continued onto sheet 2, and sheet 3 is continued onto sheet 3 or:

$$\begin{array}{ccc} 2 & 1 & 3 \\ \downarrow & \downarrow & \downarrow \\ 1 & 2 & 3 \end{array}$$

After we have determined the possible continuations, we can use numerical integration to determine if each branch covering is analytically continuous around the singular points. In order to show how this integration is effected, we use Equation (2) again and the plot shown in Figure 2. In order to check if a branch sheet in region 1 is continued onto a branch sheet in region 2 across the singular point at $1 + i$, we analytically continue the branch sheet to region 2 by integrating from point a to b in Figure 2 along the red, blue, green, yellow and purple contours. The dotted black line is the argument where all annular monodromies are taken at their associated reference point, arp. At point a in the diagram, the annular monodromy of the annulus 1 is determined. At point b , the monodromy of annulus 2 is determined. In this way we can compare the monodromies between annulus 1 and 2 to determine if a branch in region 1 analytically continues to a branch in region 2. However we cannot simply integrate from point a to b to determine this as we may be integrating too close to another singular point. Rather, we integrate over the third green leg, around the singular point to point d where we choose the radius of the green leg such that it minimizes the distance to the nearest singular point while remaining in the bordering rings. We now have integrated over an analytically-continuous route from region 1 to region 2 to point d . And our objective is to get to point b where we can compare annular monodromies. And although we could in principle integrate directly from point d to point b , we take a more symmetrical route first along the short yellow leg and then the purple leg to b . At the point b in the figure, we can compare the monodromies of

Annulus	Annulus/Singular Points	Singular Monodromy	Annular Monodromy	Branch Regions
a_1	0 {0.00005000, 0.3353} -0.2171 - 0.2555 I -0.2171 + 0.2555 I	{1}{2}{3} {{1}, {2, 3}} {{1}, {2, 3}}	{1} {2} {3}	{1} {2} {3} { r_0, r_1 } { r_0, r_1 } { r_0, r_1 }
a_2	{0.3354, 1.366} 1.366	{{1}, {2, 3}}	{1, 3, 2}	{1, 3, 2} { r_1, r_2 }
a_3	{1.366, 1.830} -1.830 - 0.020 I -1.830 + 0.020 I	{{1}, {2, 3}} {{1}, {2, 3}}	{1, 3} {2}	{1, 3} {2} { r_2, r_3 } { r_2, r_3 }
a_4	{1.831, 1.871} -1.871 1.871	{1}{2}{3} {1}{2}{3}	{1, 2} {3} ↓ {2, 3, 2} ↓ {3, 3, 3}	{1, 2} {3} { r_3, r_4 } { r_3, r_4 }
a_5	{1.871, 2.533} 2.219 - 1.222 I 2.219 + 1.222 I	{{1, 2}, {3}} {{1, 2}, {3}}	{1, 2} {3} ↓	{1, 2} {3} { r_4, r_5 } { r_4, r_6 }
a_6	{2.533, 9.147} -6.855 - 6.057 I -6.855 + 6.057 I	{{1, 2}, {3}} {{1, 2}, {3}}	{1, 2} {3}	{1, 2} { r_5, r_6 }
a_7	{9.147, 13.15}		{1} {2, 3}	{1} {2, 3} { r_6, ∞ } { r_6, ∞ }

FIGURE 3. Branch Regions for Equation 3

region 2 to those in region 1. The resulting continuations are shown in the fourth column of Figure 3 with arrows between branch regions signifying continuations.

5.7. Continuations over poles. The arrows between branches in annuli 4 and 5 in Figure 3 shows the $\{1, 2\}$ and $\{3\}$ cycles in ring 4 continued into ring 5 across two singular points. However since the intervening singular points are poles, one or more of the branch continuations may be meromorphic, that is, contain a pole. In cases involving poles, we can determine which branch sheet is affected by the pole by computing the Puiseux expansion around each singular point and then computing the value of each series at the singularity reference point c in Figure 2. We first compute the the function at point c and sort the values, then continue each branch sheet to point c and determine for each sheet, the sort order at point c . We then compute the Puiseux series at point c and then compute the value of each series at point c . Note however, the point at c for the Puiseux expansions will be offset by the singular point. For each singular point, we record the annulus, branch, sheet, singular point, sort index, the value of z at the singular point reference point, and it's offset, zP , when we translate axes to the singular point. These results are shown in Table 8. Now look at the first line in the table: We are checking the first sheet of

TABLE 8. Singular Witness Data

Line Num	Annulus	Next Cycle	Sheet	sing pt	Sort index	zstart	zP
1	4	{1,2}	1	-1.87083	2	-1.85741	0.0134149
2	4	{1,2}	2	-1.87083	1	-1.85741	0.0134149
3	4	{1,2}	1	1.87083	1	1.85741	-0.0134149
4	4	{1,2}	2	1.87083	3	1.85741	-0.0134149
5	4	{3}	3	-1.87083	3	-1.85741	0.0134149
6	4	{3}	3	1.87083	2	1.85741	-0.0134149

the 2-cycle branch $\{1, 2\}$ in annulus 4 across singular point -1.87083 and we find when we continue this branch to the singular point reference point c in Diagram 2, we find it continues onto the second root of the function at this point. The value of z at point c is -1.85741 and it's offset value around the singular

point is 0.0134149. We next compute the Puiseux expansions at this singular point:

$$\begin{aligned} w_1(z) &= (1.06397 - 1.26645i) + (3.01595 - 6.43854i)z + (0.4263 - 73.5684i)z^2 \\ &\quad - (426.834 + 907.601i)z^3 - (12030.5 + 9669.1i)z^4 - (249021. + 55181.i)z^5 + \dots \\ w_2(z) &= (1.06397 + 1.26645i) + (3.01595 + 6.43854i)z + (0.4263 + 73.5684i)z^2 \\ &\quad - (426.834 - 907.601i)z^3 - (12030.5 - 9669.1i)z^4 - (249021. - 55181.i)z^5 + \dots \\ w_3(z) &= -1.76336 + \frac{0.234968}{z} - 5.65797z - 0.676369z^2 + 853.755z^3 + 24061.1z^4 + \dots \end{aligned}$$

and then compute the value of each series at the offset point $zP = 0.0134149$:

$$\begin{aligned} w_1(zP) &= 1.10295 - 1.36858i \\ w_2(zP) &= 1.10295 + 1.36858i \\ w_3(zP) &= 15.6793 \end{aligned}$$

Now, when we compute the sorted list of the function at the point c we obtain:

$$\begin{aligned} &1.10295 - 1.36858i \\ &1.10295 + 1.36858i \\ &15.6793 \end{aligned}$$

and note $w_3(z)$ is the pole and it's value at point c is approx 15.6793 and that is the third index into the sorted list of function values at point c . Since we determined that the first sheet of branch $\{1, 2\}$ was continued onto the second index, then we know this sheet is not affected by the pole. And in the second line of the table, we see the second sheet of this branch is continued onto index 1. Therefore, since branch $\{1, 2\}$ is not continued onto the pole sheet, we know this 2-cycle branch is not affected by this singular point.

Now look at lines 3 and 4 in Table 8 as we attempt to continue the $\{1, 2\}$ cycle across 1.87083. We find at point c , the branches continue onto indexes 1 and 3. At the singular reference point for this pole (the equivalent of point c for the pole), we again compute the Puiseux series at 1.87083:

$$\begin{aligned} w_1(z) &= -0.951784 + 0.494400z - 0.146001z^2 + 0.0672361z^3 - 0.0564447z^4 + 0.0251513z^5 + \dots \\ w_2(z) &= 0.546915 - 0.405452z + 0.375163z^2 - 0.435910z^3 + 0.584467z^4 - 0.853222z^5 + \dots \\ w_3(z) &= -0.566856 - \frac{1.23497}{z} + 0.179982z - 0.377397z^2 + 0.449107z^3 - 0.571336z^4 + \dots \end{aligned}$$

and note $w_3(z)$ is the pole. When we compute the values of the series at the singular reference point we obtain:

$$\begin{aligned} w_1(zP) &= -0.958443 \\ w_2(zP) &= 0.552423 \\ w_3(zP) &= 91.4904. \end{aligned}$$

And the sorted list of function values at the witness mark is:

$$\begin{aligned} &-0.958443 \\ &0.552423, \\ &91.4904 \end{aligned}$$

so that index 3 is the pole. Thus we find the second sheet of this branch continues across this singular point but in a meromorphic fashion. When we analyze the single cycle branch in the same manner, we find it continues meromorphically across the negative pole. We identify these continuations across singular points in Table 8 as the small red monodromies along the continuation arrows. In the first case we have the second sheet of $(1, 2)$ was continuous onto the third sheet of the negative pole to the second sheet of the post annulus. This is the $(2, 3, 2)$ on the side of the first arrow. And since the single cycle branch $\{3\}$ was meromorphically continued onto the positive pole to $\{3\}$ on the post annulus, we label this as $(3, 3, 3)$ next to the continuation arrow between these branches. So that all branches in this annulus are affected

by one of the poles. Therefore the annular region of convergence of the branches in a_4 is contained in the annulus. This is shown as (r_4, r_5) below the branch monodromies in the table. And the only branch which extends beyond an annular region is branch $\{3\}$ in a_5 where it is shown to have a region of convergence (r_4, r_6) . To give a concrete example of this, the annular Puiseux series for this branch is

$$\{3\}(z) = \cdots + \frac{1.8811}{z^3} - \frac{0.9475}{z^2} + \frac{1.3012}{z} + 0.0072z - 0.00053z^2 + 0.000031z^3 + \cdots$$

and has a region of convergence of (r_5, r_7) or approximately $(1.87088, 9.1471)$.

6. COMPUTATION OF ANNULAR PUISEUX SERIES

The Newton Polygon algorithm computes power series for the function centered at a point. These power series have radii of convergences equal to the absolute value of the branch singular point which often extends only into the first few rings. In order to compute power series for the function in the remaining annular rings, we use a version of Laurent's Theorem applied to algebraic functions:

$$\begin{aligned} w_n(z) &= \sum_{k=0}^{\infty} a_k (z^{1/n})^k + \sum_{k=1}^{\infty} \frac{b_k}{(z^{1/n})^k} \\ &= A(z) + S(z) \\ a_k &= \frac{1}{2n\pi i} \oint \frac{w_n(z)}{(z^{1/n})^{k+n}} dz \\ b_k &= \frac{1}{2n\pi i} \oint w_n(z) (z^{1/n})^{k-n} dz. \end{aligned} \tag{4}$$

with $A(z)$ being the analytic terms of the series and $S(z)$, the singular terms. Or in symmetrical form:

$$\begin{aligned} a_k &= \frac{1}{2n\pi i} \oint \frac{w_n(z)}{(z^{1/n})^{k+n}} dz \\ w_n(z) &= \sum_{p=-\infty}^{\infty} a_p (z^{1/n})^p, \end{aligned} \tag{5}$$

where the integral symbol \oint indicates the integration is over a closed analytically continuous route along the integrand branch surfaces. For example, if the integrand contained a 4-cycle branch, the integration would proceed over the branch surface along an analytically continuous 8π route of winding number 4. However, we cannot simply integrate the expression as we would encounter implied branch-cuts. We can avoid this by the following derivation:

$$\begin{aligned} c_k &= \frac{1}{2n\pi i} \oint \frac{w_n(t)}{(z^{1/n})^{k+n}} dz = \frac{1}{2n\pi} \int_{t_0}^{t_e} \frac{w_n(t) r e^{it}}{(r e^{it})^{\frac{k+n}{n}}} \\ &= \frac{1}{2n\pi} \int_{t_0}^{t_e} w_n(t) (r e^{it})^{-k/n} dt \\ &= \frac{1}{2n\pi r^{k/n}} \int_{t_0}^{t_e} w_n(t) [\cos(tk/n) - i \sin(tk/n)] dt \\ &= \frac{1}{2n\pi r^{k/n}} I(k, n). \end{aligned} \tag{6}$$

From the Root Test the upper radius of convergence of the analytic terms is

$$R_a = \frac{1}{\limsup_{k \rightarrow \infty} a_k^{k/n}}$$

and the lower radius of convergence of the singular terms is

$$R_s = \limsup_{k \rightarrow -\infty} a_k^{k/n}.$$

And in order to estimate these limits numerically, we plot $\left(1/k, r\left(\frac{2n\pi}{|I(k,n)|}\right)^{n/k}\right)$, $k \neq 0$ and extrapolate to $1/k \rightarrow 0$. This will necessarily invert the expression for the upper limit so that we write the region of convergence as

$$R = \left\{ \limsup_{k \rightarrow -\infty} r\left(\frac{2n\pi}{|I(k,n)|}\right)^{n/k}, \liminf_{k \rightarrow \infty} r\left(\frac{2n\pi}{|I(k,n)|}\right)^{n/k} \right\}. \quad (7)$$

In order to demonstrate these formulas, we use

$$\begin{aligned} f(z, w) = & (-z^2 + z^3) \\ & + (-4z + 3z^2)w \\ & + (-z^3 - 9z^4)w \\ & + (-2 + 8z + 4z^2 - 4z^3)w^3 \\ & + (6 - 8z^2 + 7z^3 + 8z^4)w^4. \end{aligned} \quad (8)$$

The ring and singular points are shown in Table 9 and the continuations are in Figure 4.

TABLE 9. Rings and Singular points

Ring	Radius	Singularity	Value
r_1	0.00919971	s_1	-0.00919971
r_2	0.597463	s_2	-0.597463
r_3	0.632598	s_3	0.632598
r_4	0.692915	s_4	0.692915
r_5	0.81757	s_5	0.644655 - 0.502832 i
		s_6	0.644655 + 0.502832 i
r_6	0.85077	s_7	0.296412 - 0.797464 i
		s_8	0.296412 + 0.797464 i
r_7	0.855943	s_9	-0.0728759 - 0.852835 i
		s_{10}	-0.0728759 + 0.852835 i
r_8	0.859144	s_{11}	-0.859144
r_9	0.86077	s_{12}	-0.86077
r_{10}	0.87273	s_{13}	0.72046 - 0.492539 i
		s_{14}	0.72046 + 0.492539 i
r_{11}	0.901619	s_{15}	-0.901619
r_{12}	0.960847	s_{16}	0.859329 - 0.429862 i
		s_{17}	0.859329 + 0.429862 i
r_{13}	0.966603	s_{18}	0.966603
r_{14}	1.19237	s_{19}	-1.16276 - 0.264081 i
		s_{20}	-1.16276 + 0.264081 i
r_{15}	1.29612	s_{21}	-1.29612
r_{16}	1.30354	s_{22}	-1.30354
r_{17}	1.4026	s_{23}	0.280488 - 1.37427 i
		s_{24}	0.280488 + 1.37427 i

in the monodromy column, we see $\{2\}$ continues from the first annulus to the fourth. Therefore, the region column does not list the intervening continuations of this branch in the second third and fourth annular regions as these are part of the same $\{2\}$ branch. In the region column for this branch we have the notation $\{r_0, r_4\}$. This gives the annular region of convergence of the Puiseux expansion in terms of the ring numbers $\{r_1, r_5\}$. And from Figure 4, we see the annular domain of convergence is approximately $\{0, 0.692915\}$ which are computed from the absolute value of singular points. Likewise, the $\{4\}$ branch in annulus 3 has a region of convergence of (r_2, r_6) as it continues to the sixth annulus. This function therefore has 29 branches where we do not treat a meromorphic continuation across a pole as a single branch but rather two distinct branches.

7. USING THE ROOT TEST TO CONFIRM THE RESULTS

In order to confirm independently the convergence data in Table 4, Equation 6 was used to compute power expansions for each annular branch. Recall the symmetrical expression for the coefficients:

$$c_n = \frac{I(k, n)}{2n\pi r^{k/n}}$$

or

$$\frac{c_n}{2\pi n} = \frac{I(k, n)}{r^{k/n}}. \quad (10)$$

And consider the $(1, 2, 4)$ branch in annulus 2 with a domain $(0.009, 0.59)$ and the computation for the a_{100} term using two different values for the radius of integration and the subsequent powers:

$$\begin{aligned} 0.5^{100/3} &= 9 \times 10^{-11} \\ 0.01^{100/3} &= 2 \times 10^{-67}. \end{aligned}$$

Now, the left side of Equation 10 is a constant. So in order for the expressions to hold for $r = 0.01$ and $r = 0.5$, the integral $I(100, 3)$ would have to be much smaller for $r = 0.01$ than when $r = 0.5$, in fact, on the order of 10^{-50} . This would require a much more precise evaluation of the integral of the analytic terms when $r = 0.01$. So that we use a value of r close to the upper limit of 0.5 for the analytic terms in this case. A similar argument holds for the computation of singular terms where we have

$$\frac{c_n}{2\pi n} = I(k, n)r^{|k|/n} \quad (11)$$

so that we use a value of r close to the lower limit of 0.009.

Additionally, when the annular region extends beyond the unit circle, we are then confronted with the opposite case. Consider again the two terms:

$$\begin{aligned} 1.4^{100} &= 4 \times 10^{14} \\ 1.6^{100} &= 2 \times 10^{20}. \end{aligned} \quad (12)$$

So only a small difference results in a difference of 10^6 . So that when the domains are larger than the unit circle, we use a value of r close to the lower limit for both the analytic and singular terms.

And for regions smaller than the unit circle and when the upper and lower boundaries of the domain are similar in magnitude, calculations for the analytic power terms used a radius of integration close to the upper convergence boundary, and calculations for singular terms, a radius close to the lower boundary. In practice, these rules were adjusted by trial-and-error for best results.

We wish to numerically estimate the integral $I(k, n)$ as accurately as reasonably possible. However in many cases, the numeric estimate includes a small residual. It is therefore important to visually inspect the results and confirm the difference between the actual value of the integral and the residual is as large as possible to minimize errors.

Generally between 50 and 400 terms of each series was computed with a precision between 30 and 50 digits. The Root Test as per Equation 7 was then used to estimate the convergence domains by extrapolating the data to the point $1/n \rightarrow 0$ using the Mathematica build-in function `FindFormula`. Both Tables 10 and 11 show the percent error of the calculations as well as parameters used in the computations.

TABLE 10. Root Test Results for Singular Series

Annulus	Branch	Radius	Precision	Range	Actual	Est.	% Error
2	{1,2,4}	0.0100	30	{-100,-200}	0.009250	0.009162	0.95
3	{1,2}	0.6100	30	{-50,-100}	0.5975	0.5931	0.74
3	{4}	0.6100	30	{-50,-100}	0.5975	0.5953	0.36
4	{1}	0.6511	30	{-100,-200}	0.6326	0.6291	0.56
4	{2}	0.6387	30	{-50,-100}	0.6326	0.6303	0.36
5	{2,3}	0.7093	30	{-50,-100}	0.6930	0.6882	0.69
6	{1}	0.8209	30	{-50,-100}	0.8176	0.8174	0.024
7	{1}	0.8516	30	{-200,-400}	0.8508	0.8500	0.091
7	{4}	0.8513	30	{-200,-300}	0.8508	0.8452	0.66
8	{2,3}	0.8565	30	{-200,-400}	0.8560	0.8585	0.29
8	{4}	0.8563	30	{-200,-300}	0.8560	0.8502	0.67
9	{1,4}	0.8605	50	{-300,-600}	0.8592	0.8480	1.3
10	{2,3}	0.8620	30	{-200,-400}	0.8608	0.8527	0.95
11	{1}	0.8757	30	{-200,-300}	0.8728	0.8670	0.66
11	{2,3,4}	0.8757	50	{-300,-600}	0.8728	0.8608	1.4
12	{1,3,4,2}	0.9076	30	{-200,-400}	0.9017	0.8938	0.87
13	{1,3,4,2}	0.9615	50	{-300,-600}	0.9609	0.9468	1.5
14	{1,2}	0.9892	30	{-200,-400}	0.9667	0.9754	0.91
14	{3,4}	0.9892	55	{-400,-600}	0.9667	0.959	0.81
15	{1,3}	1.195	50	{-300,-600}	1.192	1.183	0.75
15	{2,4}	1.193	50	{-300,-600}	1.192	1.183	0.75
16	{2}	1.296	30	{-50,-100}	1.296	1.293	0.28
16	{4}	1.337	30	{-100,-200}	1.296	1.294	0.17
17	{2}	1.305	30	{-50,-100}	1.304	1.300	0.29
18	{1}	1.443	30	{-200,-300}	1.403	1.394	0.61
18	{2,3}	1.443	50	{-300,-600}	1.403	1.392	0.78

Figure 5 shows example plots of the Root Test results. Note in the figure how the lim sup of the Root Test data is used for extrapolating the singular data while lim inf used for extrapolating the analytic terms. The title for the singular plot (likewise for the analytic plot) gives the annulus and branch as $2 - (1, 2, 4)$, the region of analyticity as determined by analytic continuation as $(0.00925, 0.5974)$, radius of integration, step size and working precision of the calculations, as $0.01, (0.001, 30)$, coefficients used as $(-200, -400)$, the extrapolated value returned by `FindFormula` as 0.009175 as the percent error between the convergence value determined by analytic continuation and extrapolated Root Test.

It's important to note the plots filter out numerically imprecise values that are close to zero: In the case of the singular data, we have the expression $1/\left(\frac{c}{I(k, n)}\right)^{k/n}$. Numerical precision will however result in small residual amounts that are actually zero which in turn results in very small terms in the plot which are neglected by lim sup. A similar argument applies to the analytic terms. However this does not mean the terms can be neglected but rather are simply not included in the calculations of the Root Test.

Tables 10 and 11 summarize the results of the Root Tests. Each table lists the branch, radius of integration, working precision of the numerical integrations, coefficients used in the Root Test, and the percent error between convergence data determined by analytic continuation and extrapolated data from the Root Test. The singular table runs from annulus 2 through 18 since the first annulus has no lower limit. And the analytic table runs from annulus 1 until it reaches a branch with no upper domain limit. These are the branches with ∞ as the upper limit.

Most results agreed to within 1% error using the analysis parameters listed in each table. Figure 6 shows typical morphologies of convergence data.

TABLE 11. Root Test Results for Analytic Series

Annulus	Branch	Radius	Precision	Range	Actual	Est.	% Error
1	{1, 3}	0.009059	35	{100, 200}	0.009150	0.009225	0.83
1	{2}	0.6859	30	{50, 100}	0.6929	0.6964	0.51
1	{4}	0.009059	30	{50, 100}	0.009150	0.009231	0.89
2	{1, 2, 4}	0.5915	30	{200, 300}	0.5974	0.5940	0.57
3	{1, 2}	0.6322	35	{100, 200}	0.6325	0.6388	0.98
3	{4}	0.8482	35	{100, 200}	0.8507	0.8586	0.93
4	{1}	0.8157	30	{50, 100}	0.8175	0.8235	0.73
4	{2}	0.6923	30	{50, 100}	0.6929	0.6975	0.66
5	{2, 3}	0.8543	40	{300, 600}	0.8559	0.8631	0.84
6	{1}	0.8504	40	{200, 400}	0.8507	0.8607	1.2
7	{1}	0.8590	30	{200, 300}	0.8591	0.8675	0.97
7	{4}	0.8558	30	{50, 100}	0.8559	0.8608	0.57
8	{2, 3}	0.8607	40	{200, 300}	0.8607	0.8655	0.56
8	{4}	0.8591	30	{50, 100}	0.8591	0.8673	0.95
9	{1, 4}	0.8650	30	{200, 300}	0.8727	0.8754	0.31
10	{2, 3}	0.8726	40	{300, 600}	0.8727	0.8793	0.76
11	{1}	0.9013	30	{50, 100}	0.9016	0.9047	0.35
11	{2, 3, 4}	0.9013	35	{100, 200}	0.9016	0.8995	0.23
12	{1, 3, 4, 2}	0.9602	40	{300, 600}	0.9608	0.9657	0.51
13	{1, 3, 4, 2}	0.9665	30	{200, 300}	0.9666	0.9739	0.76
14	{1, 2}	1.190	40	{300, 600}	1.192	1.200	0.65
14	{3, 4}	1.190	40	{300, 600}	1.192	1.200	0.65
15	{1, 3}	1.400	40	{300, 600}	1.403	1.405	0.15
15	{2, 4}	1.295	35	{100, 200}	1.296	1.304	0.58
16	{2}	1.303	30	{200, 300}	1.303	1.311	0.60
17	{2}	1.402	35	{100, 200}	1.403	1.415	0.90

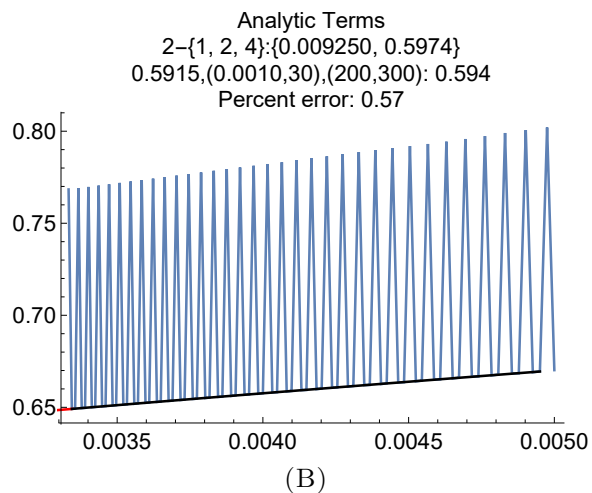
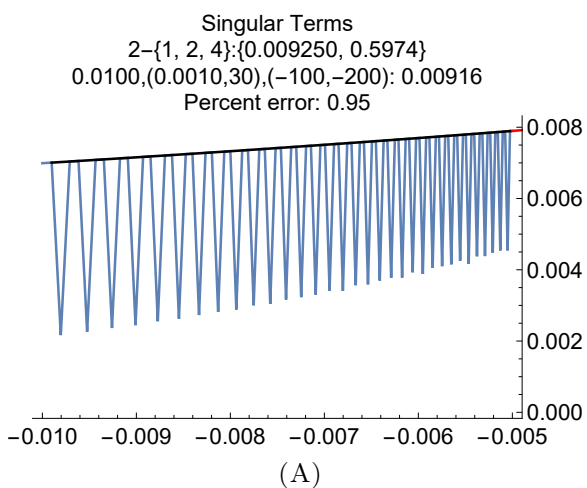


FIGURE 5. Root test results for annulus 2, branch (1, 2, 4)

Several factors affected the results of the Root Test:

- (1) Radius of Integration: The radius of integration affected the numerical precision of the results. For example, in annulus 2 branch (1,2,4). If $r = 0.5$ then the numerical precision dropped quickly for the lower limit producing poor results. However, if $r = 0.001$, then the precision stabilized and the

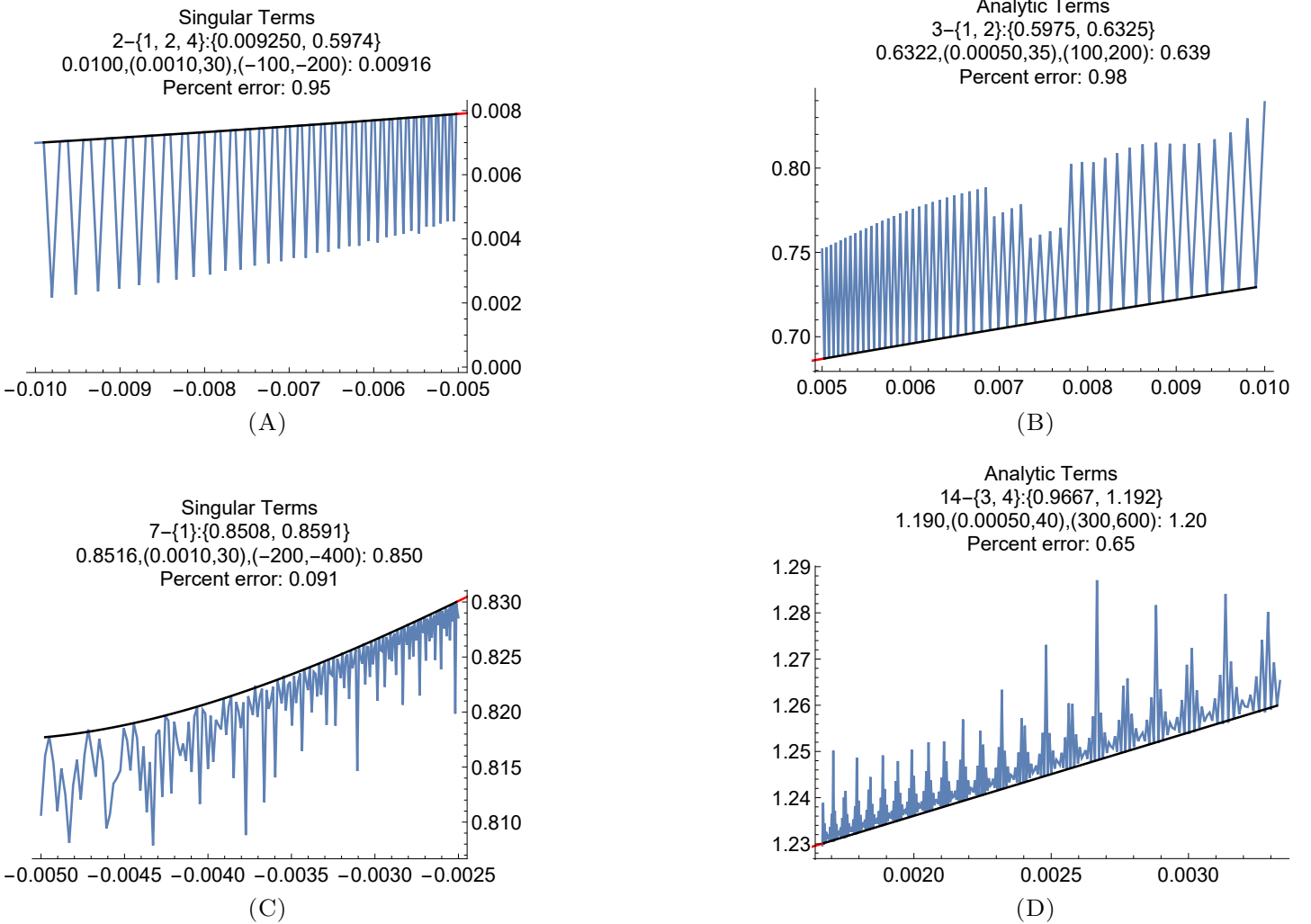


FIGURE 6. Typical convergence morphologies for Root test

data converged nicely to the expected result. Likewise, when the annular region extended beyond the unit circle, the term r^k grows very rapidly so that we use a value close to the lower limit.

- (2) A sufficient number of high-order coefficients were needed for the power series to settle down into a regular behavior: In some cases, only the first 100 terms yielded a stable converging pattern. In other cases, as many as 600 terms were used. And several test cases did not go below 1% error even after analyzing 600 terms at the level of precision used in this work.
- (3) Results depended on the working precision and step size of the integration: In this study, a maximum precision of 50 digits and step size of $1/10000$ was used.
- (4) Some coefficients of the power expansions are actually zero: Care must be taken to visually inspect the numerically-determined coefficients to decide if some terms are actually zero. Branch (4) in annulus 16 has an unbounded upper domain of convergence and all but the a_0 coefficient of the analytic terms are zero. However, due to numerical precision of the integrations, we obtain residual non-zero values for the remaining terms which grow smaller with increasing working precision. In the case of branch (2, 3) in annulus 18, all of the analytic terms are zero. This is because this (2, 3)-cycle branch is singular at infinity.

8. PLOTTING THE RESULTS

For readers interested in investigating equation 8 and its branches further, the author has a website [7] with an interactive 3D viewer. The viewer can be used to illustrate each branch. See [Algebraic Functions](#).

9. CONCLUSIONS

The branching geometry and domains determined by analytic continuation agreed well with results computed with the Root Test. At a maximum of 50 digits of precision and step size of $1/10000$, all results were in agreement below 2% error. These results suggests the analytic continuation method described above can be used to successfully determine the annular branching domains of algebraic functions of low degree, and also demonstrated the Root Test can successfully approximate the convergence domains of the associated power expansions. Care should be taken to inspect the integration results manually to confirm the integrity of the data especially since the integrands of Equation 6 become highly oscillatory with increasing k and therefore increasingly difficult to compute accurately.

REFERENCES

- [1] Bliss, Gilbert A. *Algebraic Functions*. New York: Dover Publications, Inc., 2004.
- [2] Brown, James and Ruel Churchill. *Complex Variables and Applications*. New York: McGraw Hill, 2004
- [3] Chudnovsky, D.V. and G.V. Chudnovsky. "On Expansion of Algebraic Functions in Power and Puiseux Series". *Journal of Complexity* **2**, 271-294 (1986).
- [4] Kung, H.T. and J. Traub, "All Algebraic Functions can be Computed Fast". *J. Assoc. Comput. Mach.* **25**, 245-260.
- [5] Markushevich, A.I., 1967. *Theory of Functions of a Complex Variable. Vol. III*. PrenticeHall, Englewood Cliffs, N. J.
- [6] Marsden, Jerrold and Michael Hoffman. *Basic Complex Analysis*. New York: W.H Freeman and Company, 1999.
- [7] Milioto, Dominic C. (2018, Dec. 8). Algebraic Functions, Retrieved from <http://jujusdiaries.com>.
- [8] Nowak, Krzysztof. *Some Elementary Proofs of Puiseux's Theorem*. Universitatis Iagellonicae ACTA Mathematica, Fasciculus XXXVIII, 2000.
- [9] Walker, Robert J. *Algebraic Curves*. Princeton: Princeton University Press, 1956.
- [10] Willis, Nicholas J., Didier, Annie K., Sonnanburg, Kevin M. *How to Compute a Puiseux Expansion*, arXiv: 0807.4674.1 [math.AG] 29 July, 2008

E-mail address: icorone@hotmail.com